Turkish Journal of Electrical Engineering & Computer Sciences

http://journals.tubitak.gov.tr/elektrik/

Research Article

Turk J Elec Eng & Comp Sci
(2018) 26: 1847 – 1859

doi:10.3906/elk-1703-123

Grid-connected quasi-z-source inverter with battery

Umesh SHINDE[1,*], **Sagar KOTTAGATTU**[2], **Sumant KADWANE**[2], **Snehal GAWANDE**[2]

[1]Department of Electrical Engineering, Bhivarabai Sawant College of Engineering and Research, Pune, India
[2]Department of Electrical Engineering, Yeshwantrao Chavan College of Engineering, Nagpur, India

Received: 10.03.2017 • **Accepted/Published Online:** 05.12.2017 • **Final Version:** 27.07.2018

Abstract: Grid-connected inverters are now increasingly used in distributed microgrid and smart-grid applications. The advantages of a quasi-Z-source inverter (QZSI), like single-stage operation, lower component rating, continuous input current, and common DC rail, led to an investigation of this converter for grid-connected applications. This paper presents a grid-connected QZSI with both AC and DC side controls. A new battery-charging configuration is also suggested across the capacitor through which the DC side control loop is regulated. Fast dynamic response and reduced harmonics are demonstrated through simulation and experimental results.

Key words: Quasi-Z-source inverter, distributed generation, grid-connected inverter

1. Introduction

The power converter plays a major role in photovoltaic (PV) power generation system, as it converts energy to a suitable form of energy for electrical appliances or feeding power to grid. The basic Z-source inverter (ZSI) topology and its advantages have been presented in [1]. A ZSI does not require an extra boosting device, which decreases cost, complexity, and losses in the system. The various configurations of ZSI topologies are presented and investigated in recent literature [2]. Owing to its advantages, ZSI has been a subject of much research, and therefore this converter has also been investigated for grid-connected systems [3–5]. In order to ensure the continuity of supply, a battery is also required for such applications. Such systems are a matter of interest to many researchers but have not been considered in most articles on ZSIs [6,7]. An improved ZSI has also been investigated recently, called the quasi-Z-source inverter (QZSI). QZSIs have many advantages that make them more suitable for distributed generation (DG) applications. A QZSI draws constant current from an input source, and it is also capable of handling a wide input voltage range. Currently, the control strategy for QZSIs and grid-connected systems is being analyzed [8,9]. QZSIs have been investigated for many applications, such as electric drives, battery charging, and renewable energy systems. Due to the advantages of QZSIs, researchers have also used this single-stage inverter configuration for PV systems [10,11].

QZSIs can also be used as a DC–DC converter with a cascaded switched capacitor [12] and as an AC–AC converter [13]. There are many PWM techniques for boosting the input voltage to higher values, which are discussed in [14–17]. For DC side voltage regulation, different control strategies, like sliding mode control (SMC), have also been investigated in the literature [18–20]. SMC was investigated in a grid-connected QZSI

*Correspondence: ukshinde@yahoo.com

for improving dynamic response of capacitor voltage control [21]. The superiority of SMC over a classical PI controller has been demonstrated for rapid changes in reference capacitor voltage. A new symmetrical shoot-through (SST)-based PWM technique for decoupled control of impedance source inverter was presented in [22].

For the grid-connected system, synchronization plays an important role. This can be done using a phase-locked loop (PLL). The system should maintain the power factor at unity and deliver the power to the load and the grid. The primary objective of this work is to explore the proper position of the battery for charging and to regulate the battery charging current effectively. The overall control strategy is to have appropriate DC and AC side controls for regulation of battery-charging current and AC current, respectively, irrespective of variation in the input source voltage, the required battery charging current, and the AC side current.

This paper presents a grid-connected QZSI system with closed-loop control for both the AC and DC side. A new configuration for battery charging is also recommended in this work so that the higher voltage battery can be charged with a suitable charging current, and the voltage across the capacitor can be used for charging the battery connected across it. The dynamic performance of the system is analyzed for the different changes in the system, such as input change, battery-charging current change, and AC load change. The simulation and hardware results verify the efficacy of the proposed control scheme for all the above cases. This paper presents extended work based on previous publications, with a focus on battery control circuit.

2. Circuit analysis of QZSI with battery

The proposed QZSI converter is shown in Figure 1. It contains an impedance network connected to a single-phase H-bridge inverter. The QZSI impedance network consists of inductors (L_1, L_2), capacitors (C_1, C_2), and a diode. The battery is connected across C_1. The system is designed so that the DC side control regulates the battery charging current and the AC side control regulates grid feed current, irrespective of state of charge (SOC) of battery with shoot-through–based control.

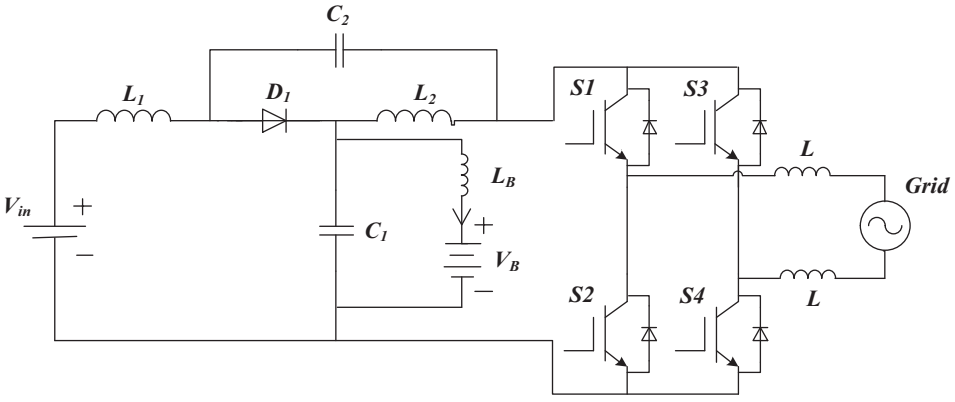

Figure 1. Grid-connected quasi-Z-source inverter.

The operation of the QZSI is as follows. For the defined range of input voltage V_{in}, the QZSI always operates in two states. One is a nonshoot–through state, and the other is a shoot-through state.

During the shoot-through state, the two switches in a single leg conduct simultaneously so that the output of the impedance network is short circuited, and the diode becomes reverse biased. This leads to the stepping-up of the input voltage, which is controlled by the shoot-through duty ratio (D).

During the nonshoot–through state, the inverter operates normally as a traditional voltage source inverter (VSI), where the two switches of one inverter leg do not operate simultaneously. Therefore, the total time period (T) will be the sum of shoot-through state time (T_0) and nonshoot–through state time $(T - T_0)$.

D can be given as $D = T_0 / T$. For a symmetrical QZS network, assuming identical values of inductances L_1 and L_2 and identical values of capacitances C_1 and C_2, the mathematical analysis of QZSI is presented as follows [8].

For the nonshoot–through state, as shown in Figure 2, the system equations can be written as

$$\left.\begin{aligned} V_{L1} &= V_{in} - V_{C1} \\ V_{L2} &= -V_{C2} \\ V_B &= V_{C1} - V_{LB} \\ i_B &= \tfrac{1}{L_B}\int_0^t V_{LB}dt \end{aligned}\right\} \tag{1}$$

$$V_{DC} = V_{C1} - V_{L2} = V_{C1} + V_{C2}, V_D = 0 \tag{2}$$

For the shoot-through state, as shown in Figure 3, the system equations can be written as

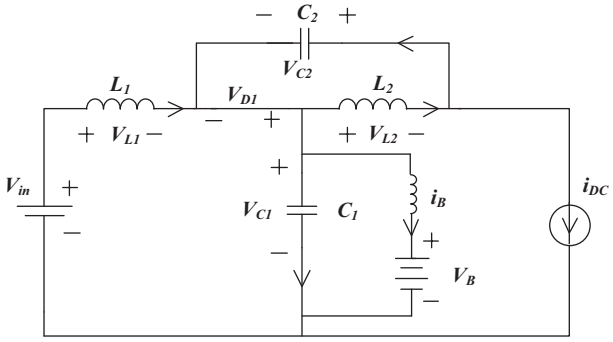

Figure 2. Quasi-Z-source inverter during non-shoot–through state.

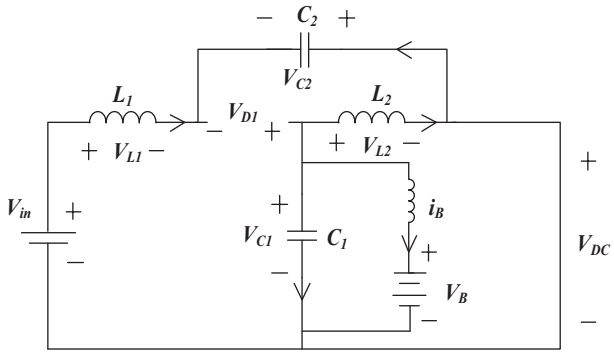

Figure 3. Quasi-Z-source inverter during shoot-through state.

$$\left.\begin{aligned} V_{L1} &= V_{C2} + V_{in} \\ V_{L2} &= V_{C1} \\ V_B &= V_{C1} - V_{LB}, \\ i_B &= \tfrac{1}{L_B}\int_0^t V_{LB}dt \end{aligned}\right\} \tag{3}$$

$$V_{DC} = 0, V_D = V_{C1} + V_{C2} \tag{4}$$

At steady state, the average voltage across the both inductors over one switching cycle is zero.

From Eqs. (1) and (3),

$$V_{L1} = \frac{T_0(V_{C2} + V_{in}) + (T - T_0)(V_{in} - V_{C1})}{T} = 0 \tag{5}$$

$$V_{L2} = \frac{T_0(V_{C1}) + (T - T_0)(-V_{C2})}{T} = 0 \tag{6}$$

Solving Eqs. (5) and (6),

$$V_{C1} = \frac{T - T_0}{T - 2T_0} V_{in} \tag{7}$$

The DC-link voltage can be given as

$$V_{DC} = V_{C1} + V_{C2} = \frac{T}{T - 2T_0} V_{in} \tag{8}$$

$$V_{DC} = \frac{1}{1 - 2D} V_{in} \tag{9}$$

$$V_{DC} = BV_{in}, \tag{10}$$

where B is the boost factor of QZSI.

Eqs. (1) to (10) demonstrate the mathematical interpretation of the proposed system. Here the voltage across the capacitor can be used to charge the batteries with the current i_B in both the shoot-through and nonshoot–through states.

3. Control strategy

The overall block diagram of the proposed grid-connected system with the control strategy is shown in Figure 4. Since the inverter output is connected to the grid, the objective of the AC side control is to regulate grid feed current, as per the reference value of the current under any disturbances in DC input voltage. The objective of DC side control is to regulate the battery-charging current in constant current mode and to regulate the voltage in constant voltage mode based on the SOC of the battery. For the power flow to the grid, the battery minimum voltage should be sufficiently high to maintain the inverter DC link voltage above the minimum required value.

For the AC side, current control is used. As per Figure 4, the unit amplitude signal has been derived from grid voltage for synchronization by using PLL. This unit amplitude signal is multiplied with the constant current reference to obtain the actual AC current reference signal. This reference AC current is compared with the actual grid current and the error signal generated is fed to the PI controller, which produces the modulating signal.

On the DC side, as the battery is connected across C_1, the current through the battery should be directed in constant current mode, and the capacitor voltage should be regulated in the constant voltage mode of the battery. In constant current mode, the actual current is compared with the current reference value and the generated error is fed to the PI controller. The PI controller produces the shoot-through signal, which is used for boosting the input voltage to higher values. The modulation signal and the shoot-through signal are logically combined by the digital controller using an SST-based PWM technique [22] and are given to the main switching controller. This modulation method achieves a sinusoidal and symmetrical distribution of shoot-through states and ensures an improved current profile, along with the capability of decoupled control for the shoot-through and the modulation index control. The AC side filter is used for suppressing harmonics.

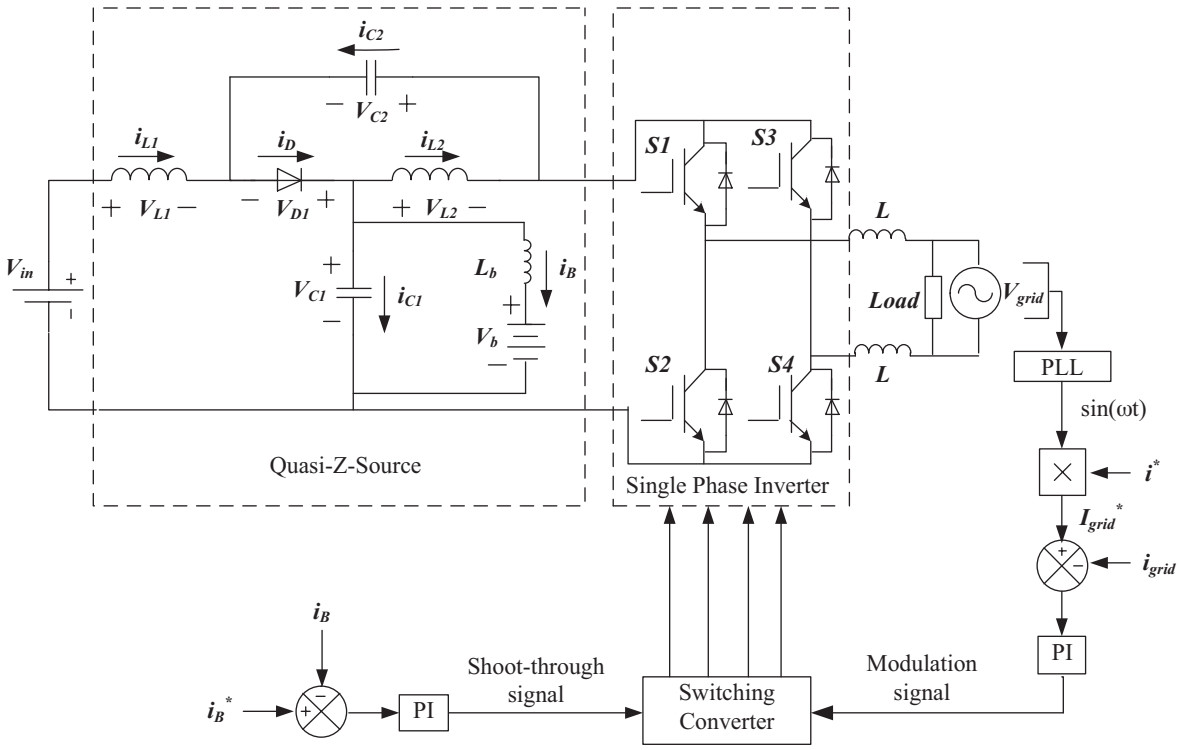

Figure 4. Proposed grid-connected quasi-Z-Source inverter with closed loop control.

4. Simulation results

The proposed system has been simulated in MATLAB/Simulink software (MathWorks, Natick, MA, USA). As QZSI is connected to the grid, it is necessary to maintain power factor at unity for feeding active power to the load and the grid. The parameter values taken for the simulation of the suggested scheme are shown in Table 1. The battery minimum voltage is 378 V and the maximum voltage is 486 V, which is sufficiently high to maintain the DC link voltage above minimum required value. The local load connected across the inverter is resistive in nature, and the active power is fed to the grid. Thus, the power factor of the power fed by the inverter is unity. Design of the PI controller and its transfer function has been carried out in accordance with [8]. PI controller parameters are as follows. For the DC side, $K_P = 0.5$, $K_I = 1$ and for the AC side, $K_P = 0.8$.

To demonstrate the steady-state response of the proposed system, the DC input voltage is kept at 250 V and the battery-charging current has been set to 10 A.

Figure 5 shows the simulated steady-state waveforms of the input voltage, capacitor voltage, battery current, grid voltage, and current, respectively. Here the battery current is regulated at 10 A and grid current is regulated at 20 A (peak).

To further analyze dynamic response of the system, a step change in input voltage is applied. Figure 6 shows the dynamic response of the system to a step change in input from 250 V to 300 V at 0.4 s. It is clear that there is no change in battery-charging current and the grid feed current waveforms, even if the input is changed. Thus the battery current and AC side current are regulated properly.

Thereafter, the dynamic response of the system to a step change in the battery charging current has been observed so as to demonstrate the effectiveness of the DC and AC side controllers. As depicted in Figure 7, the

Table 1. Specifications of simulation model of grid-connected QZSI.

Sr. No.	Parameters	Values
1	Grid Specifications	230 V, 50 Hz
2	Inverter power rating	3.5 kW
2	Switching Frequency	10 kHz
3	QZSI inductors (L_1, L_2)	160 μH
4	QZSI capacitors (C_1, C_2)	1000 μF
5	Battery series inductor (L_B)	200 μH
6	Battery bank rating	432 V, 70 Ah
7	Filtering inductor	10 mH
8	Load	R = 100 Ω, L = 100 mH

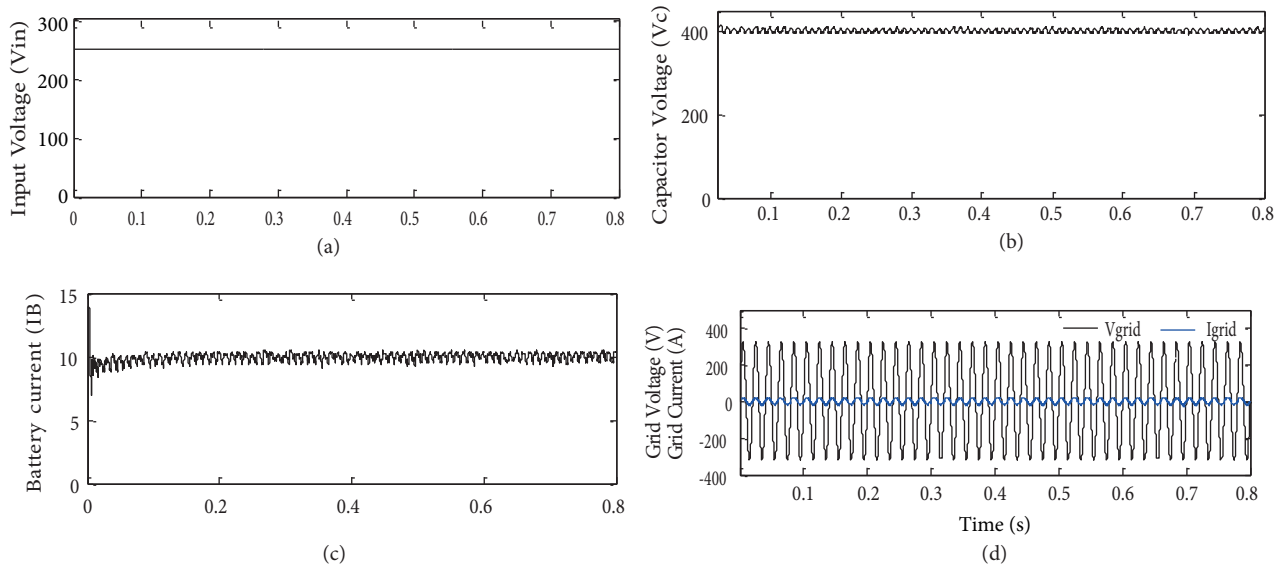

Figure 5. Simulation result for steady-state condition. (a) Input voltage. (b) Capacitor voltage. (c) Battery current. (d) Grid voltage and current.

input of the system is maintained at a constant 250 V, and the battery current is step changed from 10 A to 15 A at 0.4 s. From Figure 7, it is clear that the grid current remains unchanged, which shows that the AC and DC side controls are well designed and that synchronization with the grid is proper. As a result, the system will be more effective for the single-phase grid-connected applications.

The step change in the AC grid current from 20 A (peak) to 30 A (peak) is applied by keeping the input voltage and the battery current at 250 V and 10 A, respectively. Figure 8 shows the quick response of grid current to the change in the load at 0.5 s.

Finally, the sequential step change in input voltage at 0.3 s, AC grid current change at 0.5 s, and battery current change at 0.6 s can be observed in Figure 9. This indicates that the control is very effective and synchronization with the grid is proper.

The harmonic analysis of the proposed system is applied out to verify the harmonic content in the system. For this, various parameter changes are taken into consideration. The results of harmonic analysis

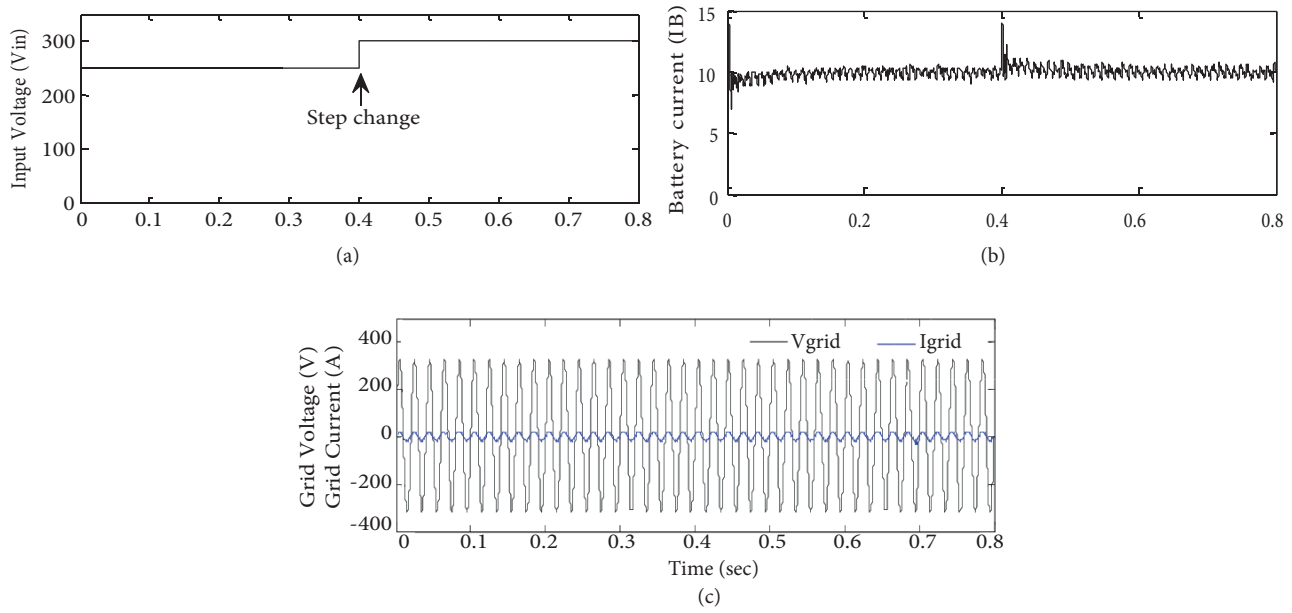

Figure 6. Simulation result for step change in input voltage. (a) Input voltage. (b) Battery current. (c) Grid voltage and current.

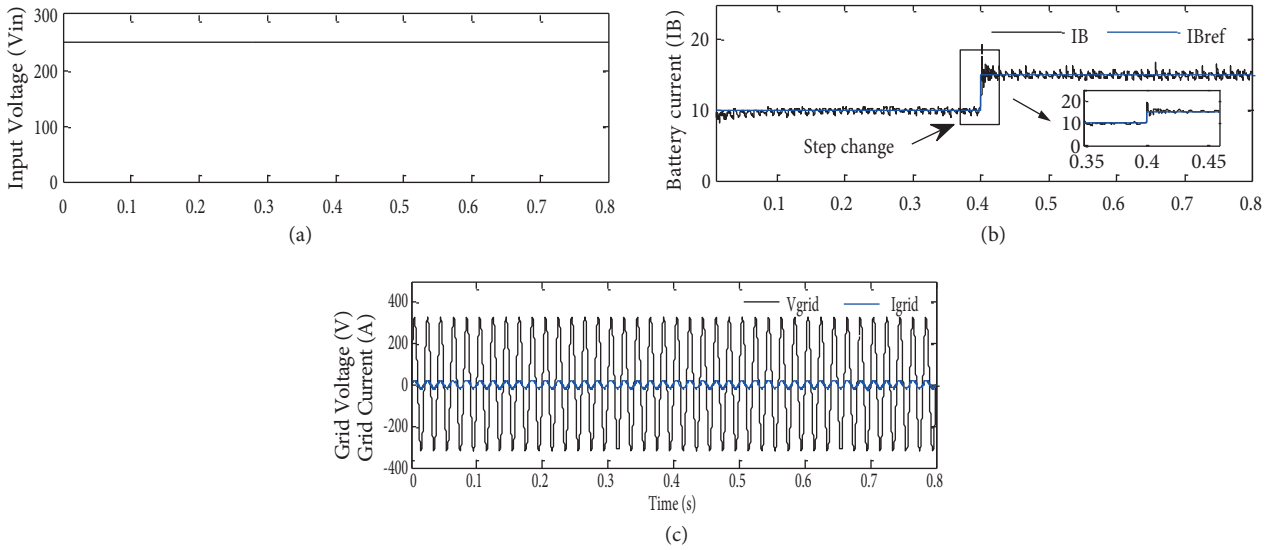

Figure 7. Simulation result for step change in capacitor voltage. (a) Input voltage. (b) Battery current. (c) Grid voltage and current.

under different input voltages and battery currents are shown in Table 2. It is clear from Table 2 that the harmonic content is within the acceptable limits.

5. Experimental results

A prototype of the QZSI system was built in the laboratory to analyze the dynamic response of the system. The system was validated for input change, battery current change, and also the AC grid feed current change. In

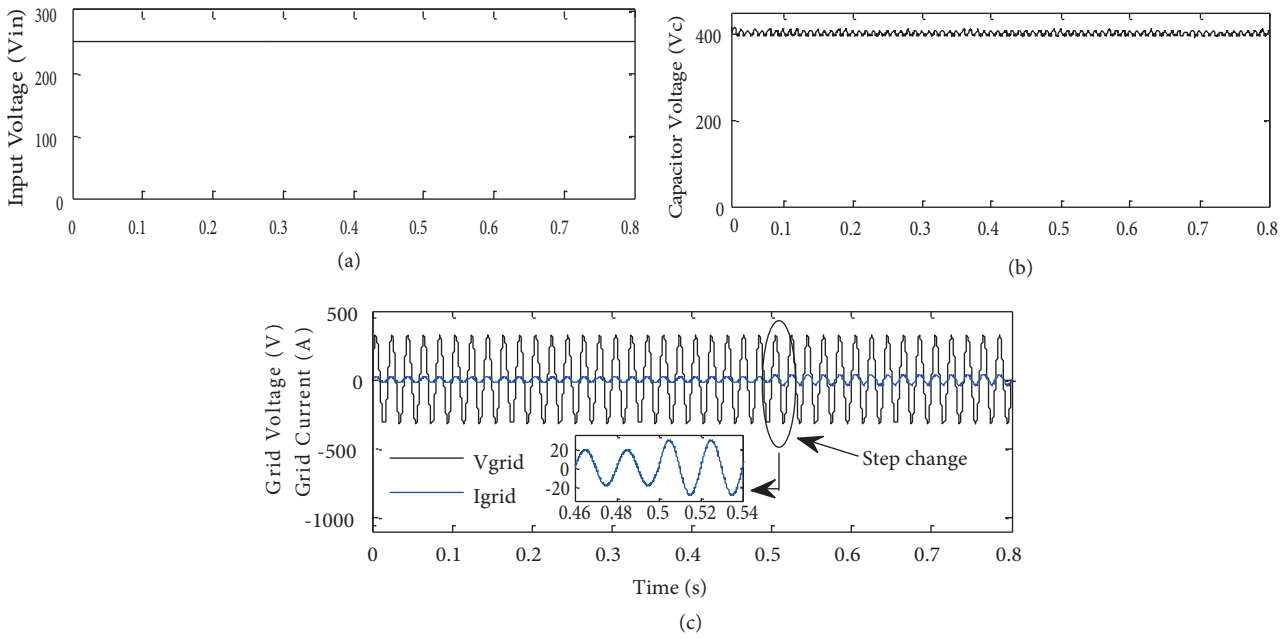

Figure 8. Simulation result for step change in load. (a) Input voltage. (b) Capacitor voltage. (c) Grid voltage and current.

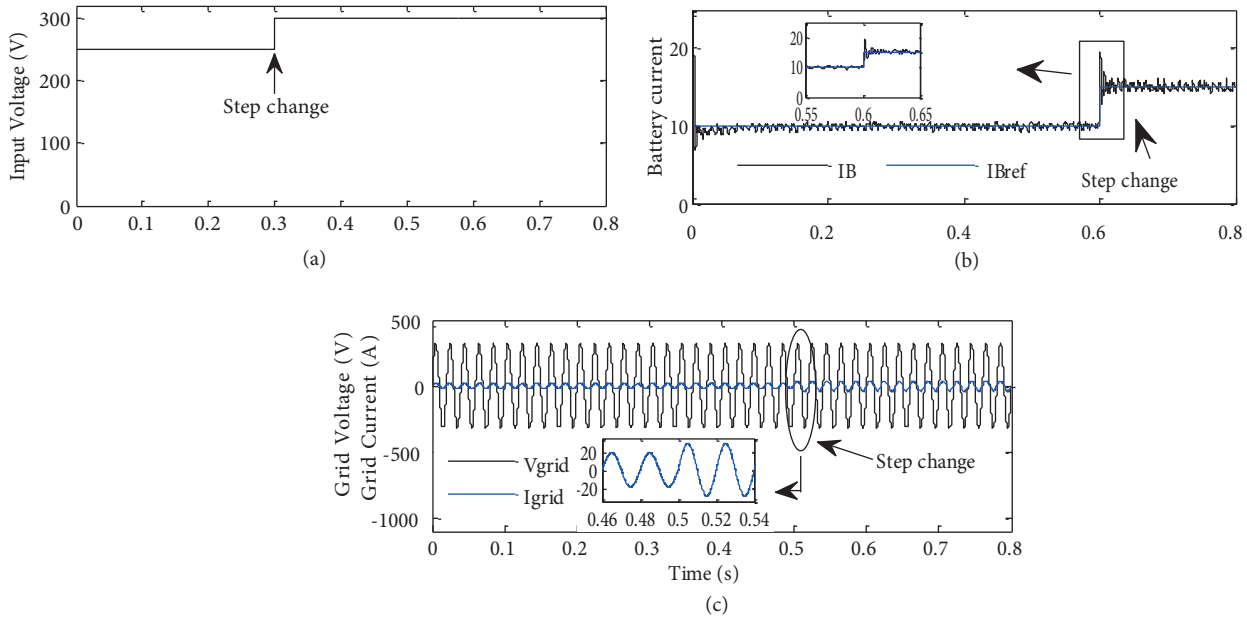

Figure 9. Simulation result for sequential change in input voltage, AC grid current, and battery current. (a) Input voltage. (b) Battery current. (c) Grid voltage and current.

the experimental setup, the system was designed for 1 kW. A total of 36 batteries of 12 V, 7 Ah were connected in series to form a battery bank of 432 V, and these were connected across C_1. The rated battery charging current was approximately 1.5 A.

Figure 10 shows the hardware setup of the QZSI system with all components. Digital controller dsPIC33EP256MC502 was used to implement the digital controller (Microchip Technology, Inc., Chandler

Table 2. Harmonic analysis under different operating conditions.

		Inverter current		Grid current	
Input voltage (V)	Battery current (A)	Fundamental (A)	THD	Fundamental (A)	THD
250	10	18.96	1.86%	16	2.23%
300	10	18.94	1.7%	15.94	2.01%
250	15	19.3	2.93%	16.36	3.45%

AZ, USA). The inverter used IGBT FGA25N120D. Four ADC measurement channels were used for battery-charging current, capacitor voltage, AC grid voltage, and grid current. The nature of pulses for upper and lower switches of both legs of the inverter is shown in Figure 11, which clearly shows the symmetrical distribution of shoot-though states.

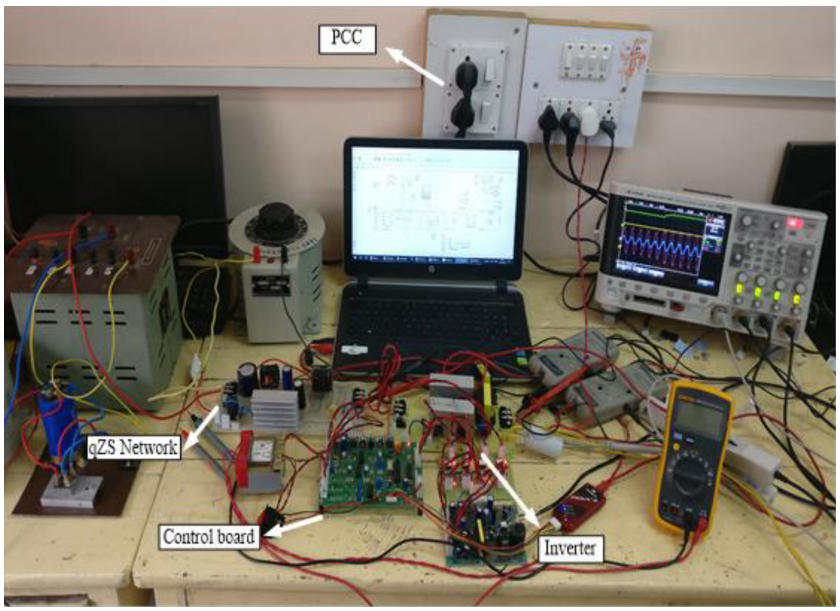

Figure 10. Photograph of hardware setup.

Experimental steady-state response of the QZSI with the input voltage (V_{in}) maintained at 250 V and the capacitor voltage (V_C) corresponding to regulated battery current at 1 A can be observed in Figures 12 and 13. The grid voltage and the current are also shown with voltage 325 V (peak) and the current 2.5 A (peak). This confirms that the steady-state response of the system and conversion of DC-AC is accurate.

The dynamic response of the proposed system is depicted in Figure 14. The input was step changed from 250 to 300 V, and the battery current was well regulated at 1 A. There was no change in grid voltage and current, which means the AC side and the DC side controls were effective and fast. So it is concluded that the system is well suited for renewable energy sources with a wide range of supply variations.

In Figure 15 the battery current was changed from 1 to 1.5 A, and the input is maintained at 250 V. The setup shows no change in the grid voltage and the current. It means that even if there are changes in the

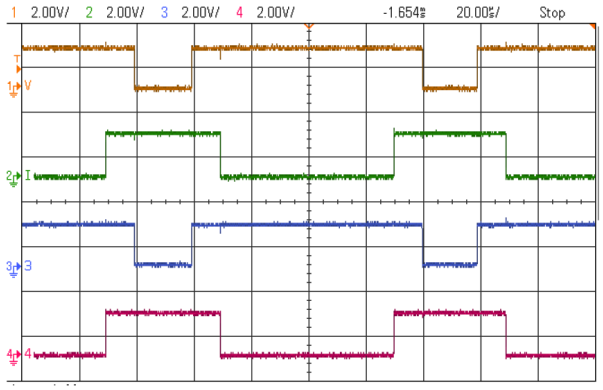

Figure 11. PWM waveforms of inverter switches (S_1, S_2, S_4, and S_3).

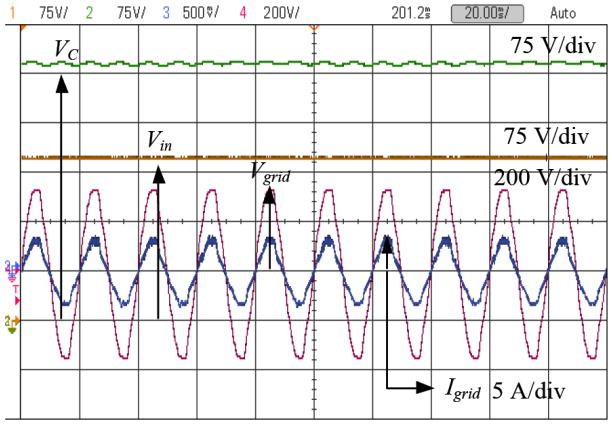

Figure 12. Experimental steady state results. (a) Input voltage. (b) Capacitor voltage. (c) Grid voltage and current.

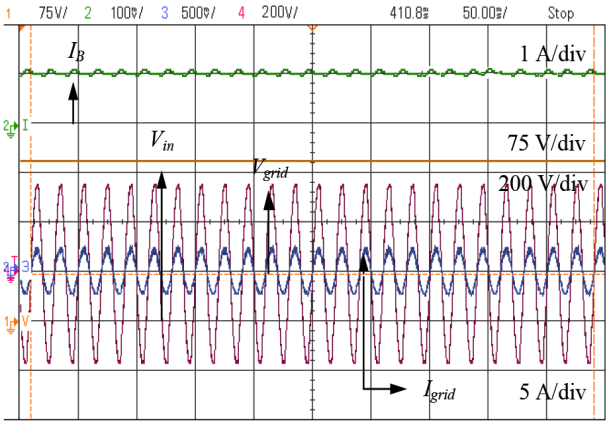

Figure 13. Experimental steady state results. (a) Input voltage. (b) Battery current. (c) Grid voltage and current.

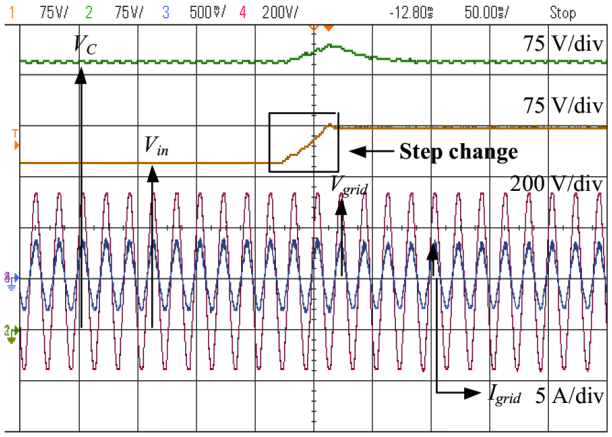

Figure 14. Experimental results for step change in input. (a) Input voltage. (b) Capacitor voltage. (c) Grid voltage and current.

battery current, it does not affect the grid voltage or the current, which shows the proper synchronization of the grid with the QZSI and disturbance rejection.

Finally, the load was changed, as shown in Figure 16, and capacitor voltage and input were maintained at a constant level. The AC side control is also proper in this case.

Figure 17 shows the steady-state experimental waveform of the inverter output voltage across switches (S_1–S_4) for an input DC voltage of 250 V. The peak voltage of the inverter output before the filter circuit is around 1.84 times the magnitude of the filtered output voltage. Therefore, the nominal voltage rating of the IGBT is suggested to be at least two times the rated output voltage of the load. The spikes across the inverter switches will lead to higher power cycles, which in turn will lead to higher temperature cycles and larger failure rates. Therefore, the precaution to be taken while selecting the inverter switches is to have a proper heat sink and a higher power rating to prevent high-voltage failure risk.

Experimental efficiency of the complete system for different battery-charging currents and inverter output currents is presented in Table 3. Figure 18 presents the plot of efficiency versus the output power of the system.

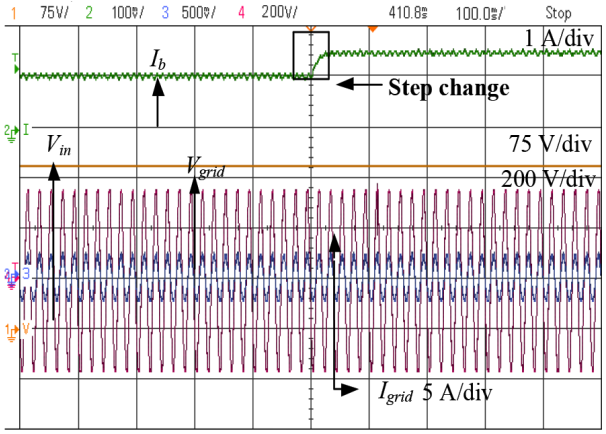

Figure 15. Experimental results for step change in reference battery current. (a) Input voltage. (b) Battery current. (c) Grid voltage and current.

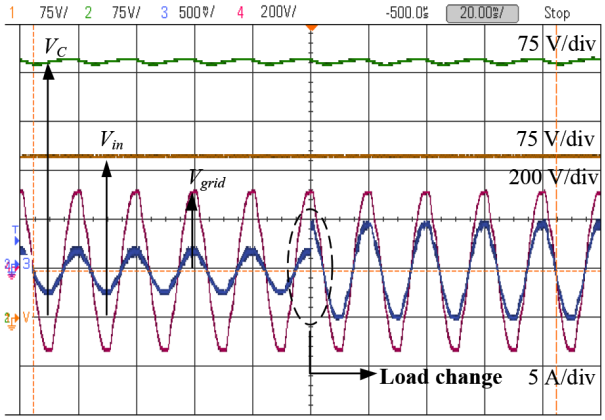

Figure 16. Experimental results for step change in load. (a) Input voltage. (b) Capacitor voltage. (c) Grid voltage and current.

The total power handled by the system is the sum of power required for battery charging and the power delivered by the inverter to the grid and/or local load.

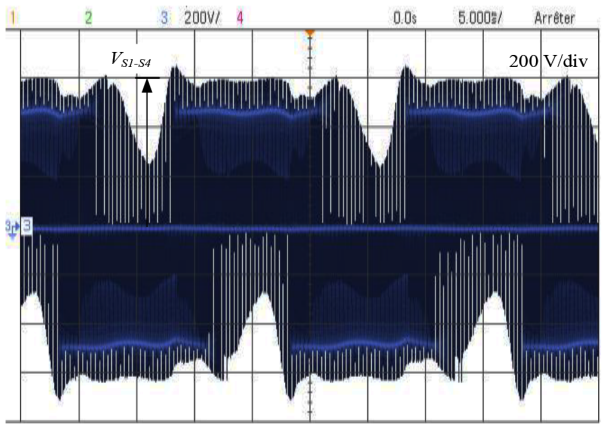

Figure 17. Experimental waveform for inverter voltage across switches (S_1–S_4).

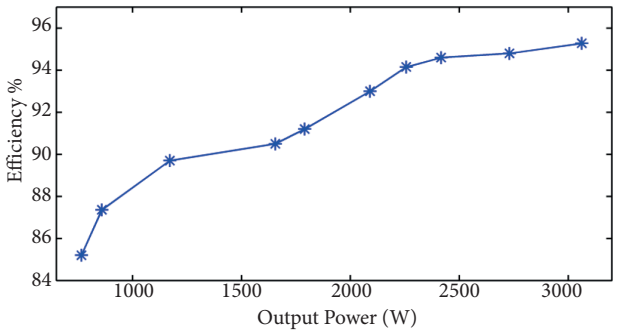

Figure 18. Experimental efficiency of the proposed system.

6. Conclusion

The effectiveness of placing a battery across C_1 is demonstrated in this paper. The proposed two-loop control strategy shows the fast tracking of the results for parameter variations. The experimental and simulation results are in agreement and prove the efficacy of the proposed system. Harmonic analysis was carried out in the simulation and THD was within limits defined by the IEEE standards. The closed loop control for both the AC and DC sides shows proper responses, and the DC link voltage is also regulated properly. The battery current is well regulated. Therefore, it is concluded that the QZSI can be easily applied to renewable energy sources where source voltage varies over a wide range. The grid-side results show proper synchronization and that the power factor is also near to unity. Therefore, it can be applied to a grid-connected system without any problems.

Table 3. Experimental efficiency of proposed system under varying load conditions.

Load	Grid	Input power	Output power	Efficiency
%	current (A)	(Watt)	(Watt)	%
100	4.3	1047	997	95.28
90	3.8	938	889	94.8
80	3.4	832	787	94.6
75	3.2	780	735	94.15
70	3	732	681	93
60	2.5	639	583	91.2
50	2.4	595	539	90.5
40	1.7	425	381	89.7
30	1.2	320	280	87.36
25	1.1	293	249	85.2

References

[1] Peng FZ. Z-source inverter. IEEE T Ind Appl 2003; 39: 504-510.

[2] Ellabban O, Abu-Rub H. Z-source inverter: Topology improvements review. IEEE Ind Electron Magazine 2016; 10: 6-24.

[3] Vinnikov D, Roasto I, Strzelecki R, Adamowicz M. CCM and DCM operation analysis of cascaded quasi-Z-source inverter. In: 2011 IEEE International Symposium on Industrial Electronics; 27–30 June 2011; Gdansk, Poland. New York, NY, USA: IEEE. pp. 159-164.

[4] Badin R, Huang Y, Peng FZ, Kim HG. Grid interconnected Z-source PV system. In: 2007 IEEE Power Electronics Specialists Conference; 17–21 June 2007; Orlando, FL, USA. New York, NY, USA: IEEE. pp. 2328-2333.

[5] Huang Y, Shen M, Peng FZ, Wang J. Z-source inverter for residential photovoltaic systems. IEEE T Power Electron 2006; 21: 1776-1782.

[6] Zhu M, Yu K, Luo FL. Switched inductor Z-source inverter. IEEE T Power Electron 2010; 25: 2150-2158.

[7] Qian W, Peng FZ, Cha H. Trans-Z-source inverters. IEEE T Power Electron 2011; 26: 3453-3463.

[8] Li Y, Anderson J, Peng FZ, Liu D. Quasi-Z-source inverter for photovoltaic power generation systems. In: 2009 IEEE Power Electronics Conference and Exposition; 15–19 February 2009; Washington, DC, USA. New York, NY, USA: IEEE. pp. 918-924.

[9] Rosas-Caro JC, Peng FZ, Cha H, Rogers C. Z-source-converter-based energy-recycling zero-voltage electronic loads. IEEE T Ind Electron 2009; 56: 4894-4902.

[10] Liu J, Jiang S, Cao D, Peng FZ. A digital current control of quasi-Z-source inverter with battery. IEEE T Ind Informatics 2013; 9: 928-937.

[11] Anderson J, Peng FZ. Four quasi-Z-source inverters. In: 2008 IEEE Power Electronics Specialists Conference; 15–19 June 2008; Rhodes, Greece. New York, NY, USA: IEEE. pp. 2743-2749.

[12] Shindo Y, Yamanaka M, Koizumi H. Z-source DC-DC converter with cascade switched capacitor. In: 2011 IEEE Industrial Electronics Society Conference (IECON); 7–10 November 2011; Melbourne, VIC, Australia. New York, NY, USA: IEEE. pp. 1665-1670.

[13] Nguyen MK, Lim YC, Kim YJ. A modified single-phase quasi-Z-source AC–AC converter. IEEE T Power Electron 2012; 27: 201-210.

[14] Tan SC, Lai YM, Tse CK. A unified approach to the design of PWM-based sliding-mode voltage controllers for basic DC-DC converters in continuous conduction mode. IEEE T Circuits and Systems I 2006; 53: 1816-1827.

[15] Shen M, Wang J, Joseph A, Peng FZ, Tolbert LM, Adams DJ. Constant boost control of the Z-source inverter to minimize current ripple and voltage stress. IEEE T Ind Appl 2006; 42(3): 770-778.

[16] Galigekere VP, Kazimierczuk MK. Analysis of PWM Z-source DC-DC converter in CCM for steady state. IEEE T Circuits Syst I Reg Papers 2012; 59(4): 854-863.

[17] Loh PC, Vilathgamuwa DM, Lai YS, Chua GT, Li Y. Pulse-width modulation of Z-source inverters. IEEE T Power Electron 2005; 20: 1346-1355.

[18] Rajaei AH, Kaboli S, Emadi A. Sliding-mode control of Z-source inverter. In: 2008 IEEE Industrial Electronics Society Conference (IECON), 10–13 November 2008; Orlando, FL, USA. New York, NY, USA: IEEE. pp. 947-952.

[19] Tan SC, Lai YM, Cheung MK, Tse CK. On the practical design of a sliding mode voltage controlled buck converter. IEEE T Power Electron 2005; 20: 425-437.

[20] He Y, Luo FL. Sliding-mode control for dc–dc converters with constant switching frequency. IEE P Control Theory Appl 2006; 153: 37-45.

[21] Shinde UK, Kadwane SG, Gawande SP, Reddy MJR, Mohanta DK. Sliding mode control of single-phase grid-connected quasi-Z-Source inverter. IEEE Access 2017; 5: 10232-10240.

[22] Kadwane SG, Shinde UK, Gawande SP, Keshri RK. Symmetrical shoot-through based decoupled control of Z-Source inverter. IEEE Access 2017; 5: 11298-11306.